Molecular Biology of the Cell
Vol. 16, 306–315, January 2005

Normal Biogenesis and Cycling of Empty Synaptic Vesicles in Dopamine Neurons of Vesicular Monoamine Transporter 2 Knockout Mice

Benjamin G. Croft,* Gabriel D. Fortin,† Amadou T. Corera,* Robert H. Edwards,‡ Alain Beaudet,* Louis-Eric Trudeau,† and Edward A. Fon*§

*Centre for Neuronal Survival and Department of Neurology and Neurosurgery, Montreal Neurological Institute, McGill University, Montreal, Quebec H3A 2B4, Canada; †Department of Pharmacology, Faculty of Medicine and Groupe de Recherche sur le Système Nerveux Central, Université de Montréal, Montreal, Quebec H3C 3J7, Canada; and ‡Departments of Neurology and Physiology, University of California San Francisco School of Medicine, San Francisco, CA 94143-2140

Submitted July 6, 2004; Accepted October 8, 2004
Monitoring Editor: Lawrence Goldstein

The neuronal isoform of vesicular monoamine transporter, VMAT2, is responsible for packaging dopamine and other monoamines into synaptic vesicles and thereby plays an essential role in dopamine neurotransmission. Dopamine neurons in mice lacking VMAT2 are unable to store or release dopamine from their synaptic vesicles. To determine how VMAT2-mediated filling influences synaptic vesicle morphology and function, we examined dopamine terminals from VMAT2 knockout mice. In contrast to the abnormalities reported in glutamatergic terminals of mice lacking VGLUT1, the corresponding vesicular transporter for glutamate, we found that the ultrastructure of dopamine terminals and synaptic vesicles in VMAT2 knockout mice were indistinguishable from wild type. Using the activity-dependent dyes FM1-43 and FM2-10, we also found that synaptic vesicles in dopamine neurons lacking VMAT2 undergo endocytosis and exocytosis with kinetics identical to those seen in wild-type neurons. Together, these results demonstrate that dopamine synaptic vesicle biogenesis and cycling are independent of vesicle filling with transmitter. By demonstrating that such empty synaptic vesicles can cycle at the nerve terminal, our study suggests that physiological changes in VMAT2 levels or trafficking at the synapse may regulate dopamine release by altering the ratio of fillable-to-empty synaptic vesicles, as both continue to cycle in response to neural activity.

INTRODUCTION

Dopamine (DA) influences behavior and is implicated in several neuropsychiatric disorders including schizophrenia, drug addiction, and Parkinson's disease. To take part in cell to cell signaling, DA, like other classical neurotransmitters, is released from synaptic vesicles (SVs) by exocytosis in response to neural activity (Greengard, 2001). One critical step in DA signaling involves the uptake of DA from the cytoplasm into SVs before release. This activity is mediated by VMAT2, the brain isoform of the vesicular monoamine transporter. Indeed, VMAT2 knockout (KO) mice are unable to store DA in SVs or to release DA in response to neural activity and, as a result, do not survive more than a few days past birth (Fon *et al.*, 1997; Takahashi *et al.*, 1997; Wang *et al.*, 1997). Mice that express only ~5% of normal VMAT2 levels are viable but show motor deficits and a reduction in both brain DA stores and synaptic release from striatal slices (Mooslehner *et al.*, 2001; Patel *et al.*, 2003). Further, even more modest changes in VMAT2 levels result in parallel changes in the quantity of DA stored within SVs and in the amount of DA released from neurons (Fon *et al.*, 1997; Pothos *et al.*, 2000). Considering that the effects of DA on neural signaling and behavior depend on the amount of DA released (Nicola *et al.*, 2000), VMAT2 expression and filling of SVs with neurotransmitter may represent a key point of regulation in DA synaptic transmission.

Synaptic vesicles cluster at the active zone in the presynaptic nerve terminal and cycle locally in order to provide an adequate reserve of SVs available for exocytosis upon high-frequency stimulation. The SV cycle involves budding from a donor compartment, docking at the active zone, fusion with the plasma membrane, endocytosis, and recycling (Hannah *et al.*, 1999). Very little is known about how these various steps in SV biogenesis and cycling relate to the filling of SVs with neurotransmitter. In a recent report, a subset of excitatory terminals in mice lacking the vesicular glutamate transporter, VGLUT1, were shown to contain fewer and irregularly shaped SVs compared with wild-type (wt) littermates, suggesting that vesicular neurotransmitter transporters are required for normal SV biogenesis (Fremeau *et al.*, 2004). However, it is not known whether a similar requirement for VMAT2 exists in DA neurons. If a

Article published online ahead of print. Mol. Biol. Cell 10.1091/mbc.E04–07–0559. Article and publication date are available at www.molbiolcell.org/cgi/doi/10.1091/mbc.E04–07–0559.

§ Corresponding author. E-mail address: ted.fon@mcgill.ca.

Abbreviations used: VMAT, vesicular monoamine transporter; DA, dopamine; SV, synaptic vesicle; KO, knockout; wt, wild-type; TEM, transmission electron microscopy; PB, phosphate buffer; TH, tyrosine hydroxylase; GLU, glutamate; VGLUT, vesicular glutamate transporter; LDCV, large dense core vesicle; NMJ, neuromuscular junction; ACh, acetylcholine; VAChT, vesicular acetylcholine transporter.

regulated sorting mechanism tightly controls the number of transporters per SV and assures the presence of at least one VMAT2 molecule per SV, then the total number of SVs in DA neurons should be intimately coupled with VMAT2 expression levels. If, on the contrary, biogenesis is independent of VMAT2, changing VMAT2 levels should not change the total number of SVs in DA neurons. In this case, with decreasing VMAT2 expression, an increasing portion of SVs would be devoid of VMAT2, unable to fill with DA, and therefore functionally "empty."

To address whether SV biogenesis and cycling are related to VMAT2 expression and SV filling in DA neurons, we have chosen to study VMAT2 KO mice. Because these mice do not express any VMAT2 protein, the characterization of SVs within their DA nerve terminals has allowed us to determine whether VMAT2 is required for SV biogenesis and cycling. Using transmission electron microscopy (TEM) in brain sections and cultured DA neurons, we show that the morphology, distribution, and numbers of SVs from VMAT2 KO mice are indistinguishable from SVs in DA neurons from wt mice. We also show, using the activity-dependent dyes FM1-43 and FM2-10, that endocytosis and exocytosis both occur in cultured DA neurons derived from VMAT2 KO mice and do so with kinetics identical to wt DA neurons, suggesting that SV cycling is independent of VMAT2-mediated filling with transmitter.

MATERIALS AND METHODS

Transmission Electron Microscopy

Tissue samples used for TEM were prepared from postnatal day 0 mice as described by Boudin *et al.* (1998), adapted for neonatal mice. Briefly, the animals were anesthetized by hypothermia followed by cardiac perfusion with 5 ml of heparin (6 U/ml in 0.9% NaCl) followed sequentially by 15 ml of a solution of 2% acrolein and 2% paraformaldehyde in 0.1 M phosphate buffer (PB), pH 7.4, and by 30 ml of 2% paraformaldehyde in the same buffer. The brains were then removed and postfixed for 30 min in the paraformaldehyde solution and then stored overnight in 0.1 M PB. The genotypes were then determined by PCR as previously described by Fon *et al.* (1997) and only the brains of VMAT2 KO and wt mice were processed further. Coronal sections (40 μm thick) of the telencephalon were cut on a vibratome and collected in PB. Sections that included the sriatum were then processed for immunogold labeling according to the protocol established by Chan *et al.* (1990) and described by Boudin *et al.* (1998), with the following changes: Rabbit anti-TH (Chemicon International, Temecula, CA, AB152) was used at a dilution of 1:1000 as the primary antibody and ultrathin sections were collected from the striatum. Samples were examined and photographed at 40,000× magnification using a JEOL 100CX electron microscope (JEOL USA, Peabody, MA), and the negatives were scanned using a Canon CanoScan N656U scanner (Lake Success, NY). A total of 6 animals, 3 VMAT2 KO and 3 wt littermates, from 3 separate litters were analyzed.

Primary midbrain cultures used for TEM were washed in 0.1 M PB and then fixed in 2% Acrolein and 2% PFA in 0.1 M PB, pH 7.4, for 20 min followed by 2% PFA in the same buffer for an additional 20 min. After fixation, the cells were treated in the same manner as the tissue sections, subsequent to the freeze-thaw step. Midbrain cultures derived from 3 VMAT2 KO from separate litters and 3 wt littermates were analyzed.

Data Analysis

The terminals of interest were selected based on the presence of three or more silver-enhanced gold particles within terminals, indicating TH immunostaining, as well as the presence of obvious synaptic densities and synaptic contact to neighboring cells. Northern Eclipse 5.0 software (Empix Imaging, Mississauga, ON, Canada) was used to examine the scanned photographic negatives of the EM samples. For the analysis of terminal area, SV numbers, size, shape and distribution, the contrast and brightness of the images were adjusted in order to optimize the resolution of cell and synaptic membranes. This effectively created high contrast images in which the membranes were very clearly defined. Single sections through terminals of interest were traced and the terminal areas were determined. SVs within the selected area were counted and marked to prevent their recounting. When comparing SV diameter, the SVs were traced and the diameter, circumference, area, and shape factor were determined by the Northern Eclipse software. The shape factor, providing a measure of SV shape, is calculated as follows: $(4 \times \pi \times \text{area})/(\text{perimeter}^2)$, with the value of a perfect circle approaching one. The averages from each group, VMAT2 KO and wt, were calculated and compared using the Student's *t* test. In determining the average diameter of the SVs, we did not correct for variability in the plane of the section through which the SVs were cut. Although this is likely to underestimate SV diameter and lead to variability in size and shape, we do not expect this to change the interpretation of our results. Indeed, these effects should be similar for the identically prepared samples from VMAT2 wt and KO mice. A similar approach was used by Van der Kloot *et al.* (2002).

Primary Midbrain Cultures

Midbrain neuron cultures used for TEM, immunocytochemistry, and FM1-43 staining were prepared as previously described (Fon *et al.*, 1997), except that the cortical astrocyte monolayers were derived from neonatal mice. The cultures used for FM1-43 staining were plated at low density (40,000 cells per well) over 40–60% confluent astrocyte monolayers and on 18-mm glass coverslips in 12-well tissue culture plates. The cultures used for immunofluorescence were derived from neonatal rats and plated at low density. All midbrain cultures were supplemented with glial-derived neurotrophic factor, (GDNF, Peprotech, 450-10, Rocky Hills, NJ) on the day of plating and were used after 3 wk in culture.

The cultures used in the FM2-10 experiments were prepared as described (Bourque and Trudeau, 2000; Bergevin *et al.*, 2002; Congar *et al.*, 2002), with a slight modification to obtain cultured neurons from individual mouse pups. Overall, the procedure involved plating neurons onto a preestablished monolayer of purified astrocytes covering a thin glass coverslip. Coverslips had first been coated with poly-L-ornithine, and then agarose, which prevents cell adhesion. Application of collagen on top of the agarose, using a microsprayer, established droplets or islands of substrate suitable for cell growth. Purified astrocytes were prepared from newborn mice and plated on the collagen droplets. The genotype of the animal used to prepare each neuronal culture was then determined using PCR on tail fragments obtained at the time of dissection. Cultures from heterozygous mice were discarded. Cultures from both VMAT2 KO and wt mice were maintained at 37°C and used between 12 and 24 d after neuronal plating.

FM1-43 Staining

Midbrain neurons, plated as described above, were viewed using a Zeiss Axiovert 200M inverted microscope with motorized stage (Carl Zeiss Light Microscopy, Göttingen, Germany). An "X," etched onto the center of the coverslip, served as a reference point for assigning coordinates to the neurons of interest. Five to 15 healthy isolated neurons were selected and photographed in phase contrast using a Retiga 1300C camera (Q-Imaging, Burnaby, BC, Canada) and Northern Eclipse 6.0 software (Empix, Mississauga, ON, Canada). The cultures were then washed once with physiological buffer (128 mM NaCl, 5 mM KCl, 2.7 mM $CaCl_2$, 1 mM $MgCl_2$, 10 mM glucose, 20 mM HEPES), and stained with FM1-43 by immersing the coverslips in a depolarizing high potassium buffer (53 mM NaCl, 80 mM KCl, 2.7 mM $CaCl_2$, 1 mM $MgCl_2$, 10 mM glucose, 20 mM HEPES) containing 15 μM FM1-43 (Molecular Probes, Eugene, OR) for 90 s, followed by three subsequent washes in physiological buffer. Previously selected neurons were then located and photographed. The neurons were then destained by depolarization in high potassium buffer for 3 min followed by immersion in the physiological buffer, and the neurons were once again photographed. The cultures were then fixed for 30 min in 4% paraformaldehyde in PBS and stored at 4°C for up to 4 d before immunostaining.

FM2-10 Staining

Neuronal cultures, prepared on 25-mm coverslips, were mounted in a closed bath imaging chamber with integrated platinum stimulating electrodes (Warner Instruments, Hamden, CT). The chamber was installed on the stage of an inverted microscope and connected to a perfusion system. Cells were then exposed for 2 min to 200 μM FM2-10 (Molecular Probes) diluted in a solution of 90 mM potassium to produce sustained membrane depolarization and exocytosis. Neurons were subsequently rinsed for 10 min in normal saline to eliminate the extracellular FM2-10 that was not internalized. Images were acquired using a point-scanning confocal microscope from Prairie Technologies LLC (Middleton, WI) and were taken every 15 s. Excitation was achieved using the 488-nm line of an argon ion laser. Emitted fluorescence was measured between 505 and 545 nm. Images were analyzed using Metamorph software v4.5 from Universal Imaging Corp (Downingtown, PA). Action potential-evoked neurotransmitter and FM2-10 release were induced by electrical field stimulation, delivered at 10 Hz (1 ms/pulse) during 60 s using a S88 stimulator from Grass Instruments (Quincy, MA). Preliminary experiments showed that the effect of the electrical stimulation was blocked by 0.5 μM tetrodotoxin, thus indicating that it induced action potentials rather than directly depolarizing axon terminals. Cells were finally exposed to high potassium saline to completely release any remaining and releasable FM2-10 from the terminals. FM2-10 fluorescence loss was quantified at individual puncta representing presumed axon terminals and was expressed relative to the average of the first eight images (2 min). Experiments were performed at room temperature.

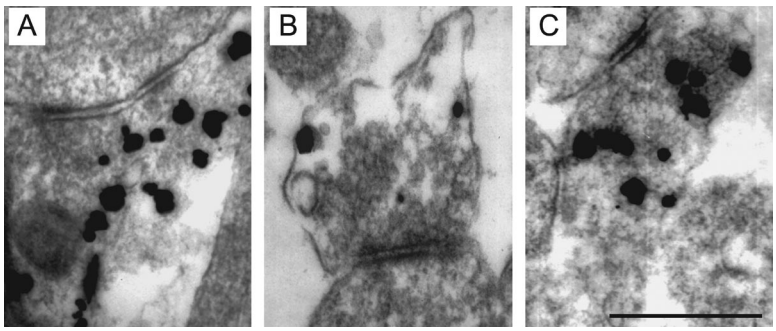

Figure 1. Ultrastructure of DA terminals and synaptic vesicles from the striatum of mice lacking VMAT2 appears normal. Representative electron micrographs from the striatum of VMAT2 KO (A and B) and wt (C) mice. The morphology of striatal DA presynaptic terminals and SVs from VMAT2 KO mice was indistinguishable from their wt littermates. Silver-enhanced gold particles indicate TH immunoreactivity, labeling DA neurons. Scale bar, 500 nm.

Immunofluorescence

After fixation, the cultured neurons were incubated for 30 min in blocking solution (3% NGS, 5% BSA, 0.1% Triton X-100 in PBS) before being incubated overnight with the Chemicon polyclonal rabbit anti-TH antibody and a monoclonal mouse antisynaptophsysin antibody (5768; Sigma-Aldrich, St. Louis, MO) diluted 1:800 in incubation buffer (0.5% NGS, 0.8% BSA in PBS). Coverslips were then washed with incubation buffer and incubated for 2 h with the secondary antibodies Cy2-conjugated donkey anti-mouse IgG and Cy3-conjugated goat anti-rabbit IgG diluted 1:2000 in incubation buffer (715-225-150 and 111-225-144; Jackson ImmunoResearch Laboratories, West Grove, PA). Finally, the coverslips were sequentially washed in incubation buffer and PBS, mounted on glass microscope slides, and examined as described above. All washes and incubations were carried out at 4°C.

Cultures used in the FM2-10 experiments were fixed with 4% paraformaldehyde for 30 min at room temperature, permeabilized with 0.1% Triton X-100 for 20 min, and bathed for 5 min in a solution containing BSA (0.5%) in order to block nonspecific binding sites. Cells were then incubated overnight at 4°C with mouse monoclonal antibodies against TH (1:5000; Pell-Freez Biologicals, Rogers, AR) and rabbit polyclonal anti-VMAT2 (Chemicon). Primary antibodies were detected using secondary antibodies coupled to Alexa-488 or Alexa-647 (1:200; Molecular Probes) before being finally mounted with Vectashield (Vector Laboratories, Burlingame, CA). Immunofluorescence images were acquired using the confocal microscope. Excitation was achieved using the 488-nm line of an argon ion laser as well as the 633-nm line of a helium neon laser.

Cultures used to assess VGLUT1 and VGLUT2 expression were washed once with cold PBS and fixed in cold methanol (−20°C) for 20 min. After washing with PBS, the coverslips were incubated 8 h in blocking solution (without Triton X-100) and processed, as described above, using polyclonal antibodies against either rat VGLUT1 or VGLUT2 (Fremeau *et al.*, 2001), diluted 1:10000 and 1:80000, respectively, as well as a monoclonal TH antibody (Chemicon International, MAB318) diluted 1:2000. Once mounted, the neurons were examined by confocal microscopy using a Zeiss LSM 510 Laser Scanning Microscope (Carl Zeiss Light Microscopy). Samples were scanned using excitation wavelengths of 543 nm and 488 nm and images were collected by dual channel recordings, with the filters adjusted to record light of wavelengths of 560 nm and over and 500–530 nm, respectively. All images were acquired with a 100× oil immersion lens.

RESULTS

Presynaptic Terminals and Synaptic Vesicles Appear Normal in DA Neurons Lacking VMAT2

To determine the effect of VMAT2 expression on the morphology of DA nerve terminals and the SVs they contain, we used TEM to examine the ultrastructure of tyrosine hydroxylase (TH) positive terminals from the striatum of newborn VMAT2 KO mice. We found that both the TH-positive terminals and SVs in the VMAT2 KO mice were similar in terms of overall morphology to those from wt littermates (Figure 1). Further, there was no difference in the surface area of TH-positive terminals despite a complete absence of synaptic DA release in the VMAT2 KOs (Figure 2A). Considering that SV numbers are reduced in glutamate terminals of VGLUT1 KO mice (Fremeau *et al.*, 2004), we asked whether the absence of VMAT2 had a similar effect on SV numbers in DA terminals. In contrast to the effects seen in the VGLUT1 KOs, we saw no difference in the total number of SVs per DA terminal (Figure 2B) or in the density of SVs within DA terminals (unpublished data) between VMAT2 KO and wt mice. In view of the evidence that the size and shape of secretory vesicles can be influenced by their level of filling (Colliver *et al.*, 2000; Fremeau *et al.*, 2004), we compared the average diameter and shape of SVs in TH-positive terminals from VMAT2 KOs to those from wt littermates. Again, we did not find any difference between the two groups in either the diameter of the SVs (Figure 2C) or in their shape (Figure 2D).

The distribution of SVs within the presynaptic terminal has been correlated with functionally defined pools of SVs. Docked SVs, which are directly apposed to the presynaptic membrane at the active zone, correspond to the readily releasable pool. Another subset of SVs that cluster near the active zone but are not docked make up the reserve pool, which can only be released after prolonged stimulation. This reserve pool together with the readily releasable pool constitute the recycling pool, defined as all the vesicles that can be labeled with lipophilic dyes, such as FM1-43, in response to extensive synaptic stimulation. An additional group of SVs that cannot take up FM1-43 has been referred to as the resting pool (Sudhof, 2000). Although intermixed with SVs in the reserve pool, vesicles in this inactive resting pool tend to cluster further away from the active zone (Schikorski and Stevens, 2001). Given that the SVs in the DA neurons of VMAT2 KO mice do not contain DA and therefore do not participate in DA neurotransmission, we were interested in determining their distribution within the nerve terminal. Using TEM, we found no differences between VMAT2 KO and wt mice in the numbers of vesicles that were docked, in those that were between 50 and 150 nm from the active zone (i.e., close to, but not touching the presynaptic membrane), or in those that were further than 150 nm from the active zone (Figure 2E). We similarly analyzed the size of SVs according to their distribution within the terminals and again, we found no differences between the terminals from VMAT2 KO and those from wt mice (Figure 2F).

Together, these results indicate that DA neurons in VMAT2 KO mice developed morphologically normal synapses with normal SVs, distributed in a manner suggesting that they are capable of undergoing normal SV cycling. This prompted us to examine more directly whether or not the SVs do indeed cycle. As this required the use of cultured DA neurons, we first needed to establish that cultured midbrain DA neurons lacking VMAT2 were also ultrastructurally indistinguishable from wt, as we had observed in tissue sections in vivo. To this end, we prepared primary midbrain cultures from VMAT2 KOs and their wt littermates, processed them for TEM, and analyzed them as we had for the tissue samples. As was the case for the striatal tissue sections, we found no differences between VMAT2 KO and wt neurons (Figure 3), either in the average terminal area, the

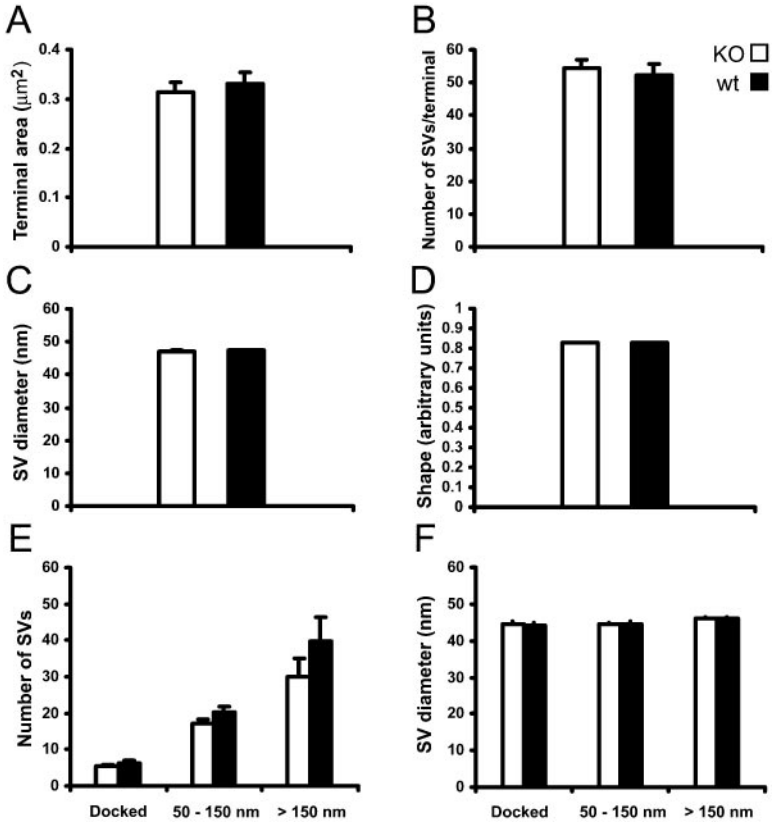

Figure 2. Striatal DA presynaptic terminals and synaptic vesicles are morphologically normal in mice lacking VMAT2. No differences were observed between the VMAT2 KO and wt samples when the ultrastructural features of presynaptic DA terminals were examined. (A) Average area of single sections through TH-positive, presynaptic terminals (VMAT2 KO : 0.314 ± 0.021 μm^2, n = 78; wt: 0.330 ± 0.025 μm^2, n = 77; not significant [ns]; values represent the mean ± SE of the mean [SEM]); (B) average total number of SV per terminal (VMAT2 KO: 54.3 ± 2.5 n = 78 terminals; wt: 52.2 ± 3.4, n = 77 terminals; ns); based on single sections through individual terminals; (C) average SV diameter (VMAT2 KO : 46.93 ± 0.43 nm, n = 148 SVs; wt: 47.30 ± 0.35 nm, n = 147 SVs; ns); (D) average shape factor of SVs (VMAT2 KO: 0.828 ± 0.002, n = 148 SVs; wt: 0.828 ± 0.002, n = 147 SVs; ns); (E) distribution of SVs at the active zone (VMAT2 KO: 5.6 ± 0.4 docked SVs, 17.3 ± 1.2 SVs between 50 and 150 nm of the active zone and 29.9 ± 5.2 SVs >150 nm from the active zone, n = 15 terminals; wt: 6.3 ± 0.8 docked SVs, 20.2 ± 1.6 SVs between 50 and 150 nm of the active zone and 39.8 ± 6.6 SVs >150 nm from the active zone, n = 15 terminals; ns); (F) SV size according to SV distribution (VMAT2 KO: docked SVs = 44.60 ± 0.70 nm, SVs between 50 and 150 nm of the active zone = 44.35 ± 0.54 nm, SVs >150 nm from the active zone = 45.95 ± 0.57 nm, n = 5 terminals; wt: docked SVs = 44.05 ± 0.91, SVs between 50 and 150 nm of the active zone = 44.58 ± 0.77, SVs >150 nm from the active zone = 46.04 ± 0.53, n = 5 terminals; none of the groups were significantly different from one another); error bars, SEM.

total number of SVs per terminal, the average SV diameter or in the distribution of SVs within the terminals (Table 1). The remarkable conservation of ultrastructural parameters between DA nerve terminals in striatal brain sections and those in culture validates our use of the cultured midbrain neurons to examine the effects of VMAT2 on SV cycling.

Vesicular Glutamate Transporters Are not Colocalized with TH in Cultured Midbrain DA Neurons

When cultured in isolation, midbrain DA neurons have been reported to both express VGLUT2 and corelease the neurotransmitter glutamate in addition to DA (Sulzer *et al.*, 1998; Dal Bo *et al.*, 2004). We therefore examined whether the TH-positive varicosities in DA neurons in our cultures also expressed VGLUT2. The VGLUT2 antibodies specifically labeled the majority of neurons cultured from rat hippocampus, a rich source of glutamate neurons. In these cultures, VGLUT2 labeling was punctate and colocalized extensively with synaptophysin, demonstrating the specificity and the sensitivity of the VGLUT2 antibody (unpublished data). In contrast, in our midbrain cultures, ~30% of the neurons stained for TH, whereas <5% of the neurons were positive for VGLUT2 (n = 6 coverslips from 3 independent cultures). More importantly, VGLUT2 staining did not colocalize with the TH immunoreactivity in any of the neurons examined, as determined by confocal microscopy (Figure 4, A–C). Although we cannot completely exclude that these neurons corelease DA and glutamate, the data suggest that, at least in the majority of cases, glutamate is not coreleased from the same TH-immunoreactive terminals as DA. This finding fits well with our recent work showing that the ability of cultured DA neurons to express VGLUT2 is partially repressed when DA neurons are in contact with other neurons (Dal Bo and Trudeau, unpublished results), as is the case in our mixed cultures. Moreover, even in isolated DA neuron cultures, TH-positive and VGLUT2-positive terminals are partially segregated (Dal Bo *et al.*, 2004). In contrast to VGLUT2, cultured midbrain DA neurons have not been shown previously to express other VGLUT isoforms. Nonetheless, as an additional control, we also determined that VGLUT1 did not colocalize with TH in our cultures. Similarly to our findings with VGLUT2, the VGLUT1 antibody specifically stained rat hippocampal neurons and the staining was punctate and colocalized extensively with synaptophysin (unpublished data). In the midbrain cultures, however, VGLUT1 staining was detected in <1% of the neurons and did not colocalize with TH immunostaining (Figure 4, D–F; n = 6 coverslips from 3 independent cultures). Taken together, these data indicate that glutamate is unlikely to be coreleased with DA from TH-positive terminals in our cultures. Importantly, this further supports the notion that SVs in TH-positive terminals from the VMAT2 KO mice are unable to fill with either DA or glutamate and are therefore likely functionally empty.

DA Neurons Lacking VMAT2 Display Activity-dependent Synaptic Vesicle Cycling

Having established that SVs in TH-positive terminals lacking VMAT2 were distributed in a manner that suggested SV cycling and that they were unlikely to be filled with glutamate, we went on to determine directly whether they were able to undergo endocytosis and exocytosis in response to membrane depolarization. First, we assayed SV cycling using the lipophilic styryl dye FM1-43 (Figure 5). FM1-43, although unable to pass through the plasma membrane, reversibly inserts into the membrane where it fluoresces

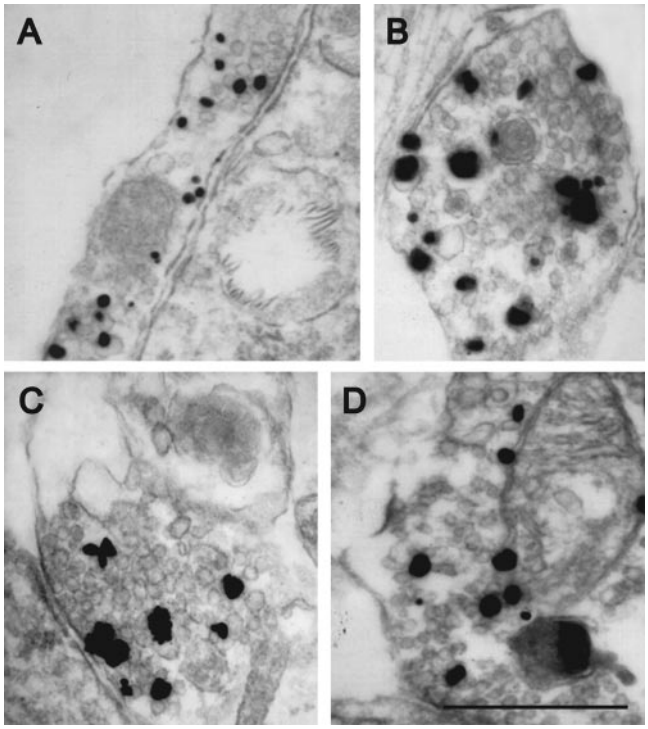

Figure 3. Ultrastructure of synaptic terminals and synaptic vesicles appears normal in DA neurons cultured from mice lacking VMAT2. Representative electron micrographs from midbrain cultures generated from VMAT2 KO (A and B) and wt (C and D) mice. As in the case of the striatal tissue sections, the ultrastructure of TH-positive presynaptic terminals from VMAT2 KO mice was indistinguishable from those derived from wt littermates. Silver-enhanced gold particles indicate TH immunoreactivity, labeling DA neurons. Scale bar, 500 nm

intensely and can readily be washed off. FM1-43 can be internalized during endocytosis and results in punctate fluorescent staining in live cells at the site of SV cycling. Similarly, FM1-43 can be released from SVs when they undergo exocytosis (Cochilla *et al.*, 1999).

When we depolarized neurons within the midbrain cultures with 80 mM KCl for 90 s in the presence of FM1-43 and then washed off the dye using physiological buffer, FM1-43 was detectable within varicosities, indicating that endocytosis had taken place in response to depolarization, in both VMAT2 KO (Figure 5, Ab and Ba) and wt (Figure 5, Ah and Bc) neurons. Subsequently, we stimulated the cultures with KCl again, but in the absence of FM1-43, to induce exocytosis and the release of the dye. The same neurons showed a clear decrease in FM1-43 fluorescence, approaching the level of background fluorescence, indicating that SVs in both VMAT2 KO (Figure 5, Ac and Bb) and wt (Figure 5, Ai and Bd) neurons had undergone exocytosis in response to the second depolarization.

The midbrain cultures that we use typically contain ~30% TH-positive DA neurons, whereas the other neurons in the culture are mainly GABAergic (Rayport *et al.*, 1992). To determine whether the endocytosis, exocytosis, and SV cycling we observed occurred specifically in TH-positive neurons, we fixed the cultures immediately after the FM1-43 assay and immunostained them using antibodies against TH and synaptophysin. We analyzed only neurons that we had retrospectively determined to be TH-positive (Figure 5, Ad and Aj) and considered only those that were clearly isolated from other neurons. To further verify that FM1-43 staining corresponded to SV cycling within the DA neurons, we determined the distribution of synaptophysin, an SV protein that serves as a presynaptic marker and whose expression has been shown to correlate to the extent of FM1-43 uptake (Staple *et al.*, 1997). Indeed, synaptophysin colocalized to TH-positive cells and localized extensively to the areas that had been stained with FM1-43 (Figure 5, Ae, Af, Ak, and Al). We analyzed FM1-43 uptake in a total of 78 TH-positive neurons from 11 cultures derived from three separate VMAT2 KO mice and 32 TH-positive neurons from five cultures derived from three separate wt littermates and noted consistent results in each of the cultures.

To ensure that the observed FM1-43 staining and destaining was specific and activity dependent, we performed the following control experiments: First, in a mock-staining experiment, we exposed cultures to FM1-43 in the presence of physiological buffer and observed no specific staining (Figure 6A). Second, we washed an FM1-43–stained culture with physiological buffer instead of the second depolarization, to ensure that no significant bleaching or nonspecific dye release was occurring (mock destain), and there was no decrease in FM1-43 staining (Figure 6B). Finally, we verified that the fluorescence observed after immunostaining was not due to residual FM1-43, which was eliminated by the fixation and permeabilization process (Figure 6C).

To further characterize the kinetics of SV cycling in DA neurons from VMAT2 wt and KO mice, we used FM2-10. FM2-10 is a styryl dye, similar to FM1-43 but with faster binding and unbinding kinetics, thereby providing a higher temporal resolution when monitoring SV cycling. Confocal

Table 1. Morphometric analysis of cultured midbrain DA neurons form VMAT2 KO and wt mice

	VMAT2 KO	wt
Terminal area (μm^2)	0.504 ± 0.033^a	0.442 ± 0.032^b
Number of SVs per terminal	48.7 ± 3.3^a	51.3 ± 3.2^b
Number of docked SVs	7.8 ± 0.7^c	7.6 ± 0.6^d
Number of SVs between 50 and 150 nm from active zone	14.8 ± 1.2^c	15.1 ± 1.3^d
Number of SVs greater than 150 nm from active zone	34.7 ± 4.1^c	45.0 ± 7.5^d
Vesicle diameter (nm)	46.68 ± 0.38^e	46.27 ± 0.37^f

No differences were observed in the ultrastructural features of TH-positive terminals between neurons cultured from VMAT2 KO and wt mice. Numbers indicate mean ± SEM.

[a] n = 86 terminals; [b] n = 90 terminals; [c] n = 20 terminals; [d] n = 20 terminals; [e] n = 210 SVs; [f] n = 195 SVs. None of the values showed statistically significant differences between VMAT2 KO and wt.

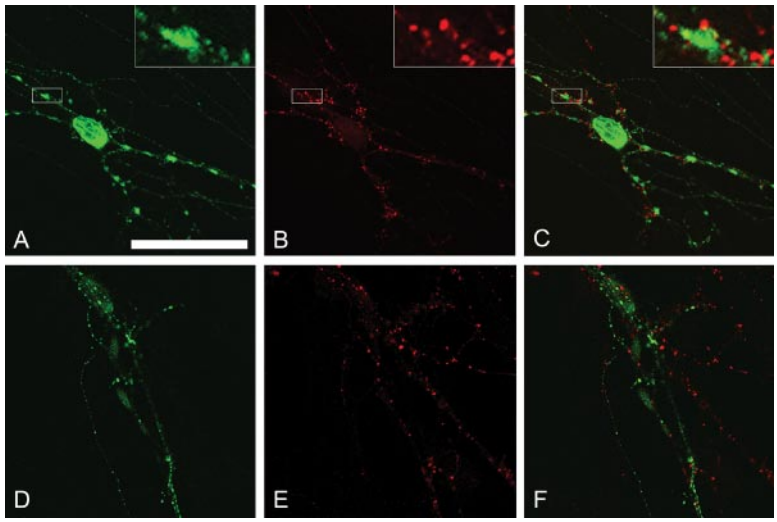

Figure 4. VGLUT1 and VGLUT2 are not colocalized with TH in cultured midbrain neurons. Representative images of midbrain cultures stained for TH (A and D), VGLUT2 (B), and VGLUT1 (E) showing that TH-positive processes do not express VGLUT2 or VGLUT1. This suggests that the SVs observed in the VMAT2 KO neurons are not filling with glutamate. (C) Merge of A and B; (F) merge of D and E. Scale bar, 20 μm.

imaging experiments were performed on isolated neurons from "μ-dot" cultures. In this model, cultured neurons grow alone or with a small number of other neurons on small dots of substrate. Under such conditions, isolated neurons can be found establishing functional synaptic connections onto themselves (Bekkers and Stevens, 1991; Sulzer *et al.*, 1998; Michel and Trudeau, 2000; Congar *et al.*, 2002), thus permitting the study of axonal terminals belonging to a single neuron. Neuronal phenotypes were determined by post hoc TH-immunostaining as above. To examine whether the rate of SVs cycling was affected by the absence of VMAT2, we quantified the level of FM2-10 staining and the rate of destaining from four wt neurons and five VMAT2 KO neurons and found no significant difference in the rate at which neurons from either group destained (Figure 7).

Taken together, these experiments show that both the qualitative and quantitative parameters of activity-dependent exocytosis and endocytosis of SVs in DA neurons from VMAT2 KO mice are indistinguishable from those of wt mice, indicating that empty, synaptically nonfunctional SVs cycle normally.

DISCUSSION

In this study, we have established that SVs devoid of VMAT2 are indistinguishable from those that bear VMAT2. In a previous study, we showed that both the DA neuron cell bodies in the midbrain and their projections in the striatum appear normal in VMAT2 KO mice at the level of light microscopy (Fon *et al.*, 1997). Further, we demonstrated that although DA is produced within the brains of VMAT2 KO mice, it is not stored in SVs and is rapidly degraded in the cytoplasm. Similarly, midbrain neuron cultures form these mice do not store or synaptically release any DA. We are therefore confident that the SVs in the VMAT2 KO mice that we examined at the ultrastructural level in this study are unable to fill with DA and are thereby functionally "empty."

Under certain circumstances, cultured midbrain neurons have been reported to both express VGLUT2 and corelease glutamate along with DA (Sulzer *et al.*, 1998; Dal Bo *et al.*, 2004). In addition, glutamate-mediated synaptic responses have been detected in striatal neurons after extracellular stimulation of DA neurons in a mouse brain slice preparation (Chuhma *et al.*, 2004). These findings raise the possibility that the SVs observed in the VMAT2 KO samples are filled with glutamate. However, despite the detection of low levels of VGLUT3 mRNA by in situ hybridization in one study (Fremeau *et al.*, 2002), none of the VGLUTs have been detected in vivo in DA neurons at the protein level (Fremeau *et al.*, 2001, 2002; Herzog *et al.*, 2001; Gras *et al.*, 2002; Schafer *et al.*, 2002; Varoqui *et al.*, 2002; Herzog *et al.*, 2004). Further, even in cultured DA neurons, it appears that glutamate and DA are released from different terminals (Sulzer *et al.*, 1998; Dal Bo *et al.*, 2004). Consistent with this, we did not detect VGLUT immunoreactivity in TH-positive varicosities in our cultures. Further, our preliminary analysis indicates that VGLUT2 is not up-regulated in TH-positive neurons in cultures from VMAT2 KO mice (Fortin and Trudeau, unpublished results). Therefore, considering that our criteria for selecting terminals for electron microscopy, FM1-43 and FM2-10 was based on TH immunostaining, it is likely that the majority of the terminals that we analyzed would not have had the capacity to release glutamate.

We found that the morphology of SVs is unaffected by the absence of VMAT2. In contrast, Colliver *et al.* (2000) demonstrated that large dense core vesicles (LDCVs) in PC12 cells varied in size according to the extent to which they were filled. Although both LDCVs and SVs can bear VMAT2 and take up monoamines, they differ considerably. LDCVs are formed at the level of the Golgi and are then trafficked to the plasma membrane throughout the cell whereas SVs cycle locally, principally at axonal varicosities and synaptic terminals (Hannah *et al.*, 1999). Given the fundamental differences between these vesicle types, it is not surprising that their transmitter content could influence their morphology differently. Further, LDCVs were relatively rare in our samples and VMAT2 is predominantly expressed on SVs in DA terminals in brain (Nirenberg *et al.*, 1997). Therefore, we did not analyze the LDCVs in our samples. The diameter of SVs has also been shown to vary along a narrow distribution curve (Bekkers *et al.*, 1990; Zhang *et al.*, 1998; Bruns *et al.*, 2000). In serotonin (5-HT) releasing leech Retzius neurons, the variability in SV diameter correlates with the variability in the amount of transmitter released by individual SVs (Bruns *et al.*, 2000). However, this association appeared to reflect that SV size determined transmitter content rather than the contrary. Further, a recent study by Van der Kloot *et al.* (2002) supports our finding that SV morphology is independent of SV filling. The authors determined that, at the frog neuromuscular junction (NMJ), SV size remained

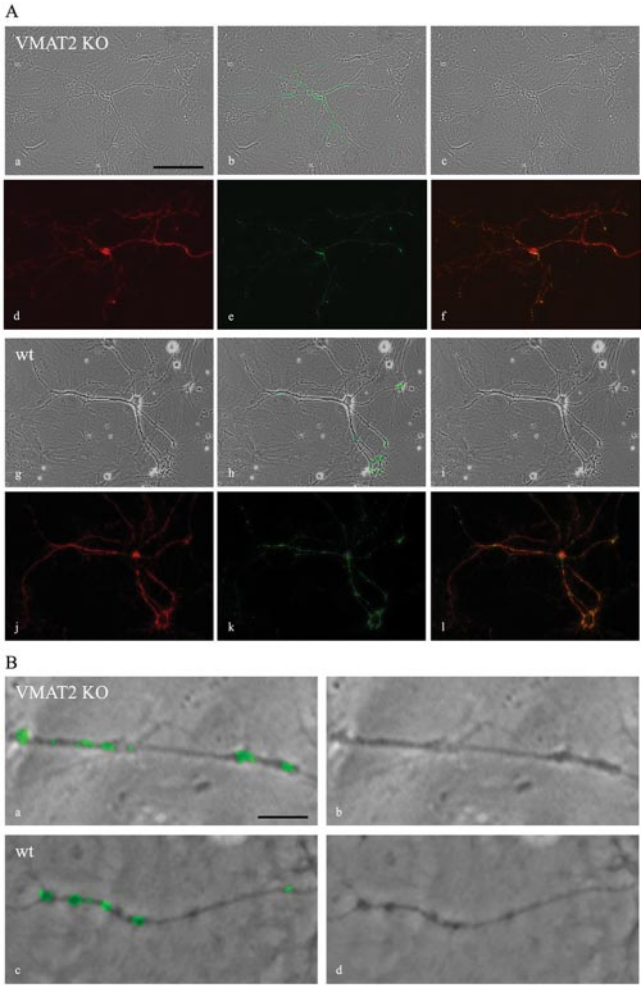

Figure 5. DA neurons lacking VMAT2 display synaptic vesicle exocytosis and endocytosis. (A) Representative images of FM1-43 staining of a cultured neuron derived from a VMAT2 KO (a–f) and from a wt littermate (g–l) showing that the SVs of TH-positive cultured midbrain neurons cycle in an activity-dependent manner despite being unable to fill with transmitter. (a and g) Phase contrast image of live neurons. (b and h) Image from panel a or g, respectively, with an overlaid pseudocolor fluorescent image of FM1-43 staining. (c and i) Image from panel a or g, respectively, with an overlaid pseudocolored image of the same neuron after FM1-43 destaining. After staining and destaining, the cultures were fixed and immunostained for TH (d and j) and synaptophysin (e and k). (f and l) The merged images of d and e and j and k, respectively (TH in red and synaptophysin in green). Synaptophysin staining colocalizes with TH-positive neurons and localized extensively to areas of FM1-43 uptake. Scale bar, 100 μm. (B) Higher magnification images of single neurites from TH-positive neurons derived from a VMAT2 KO (a and b) and a wt mouse (c and d) showing stimulation dependent FM1-43 staining (a and c) and destaining (b and d). Scale bar, 10 μm. Note that the FM1-43–stained and –destained images were processed identically to one another for each field: the pseudocolored overlays were generated by highlighting all fluorescence brighter than a threshold set slightly above the background fluorescence of the FM1-43–stained image.

constant throughout manipulations that significantly altered quantal size.

Perhaps of greater significance is our finding that not only is the morphology of SVs normal in DA neurons of VMAT2 KO mice, but that their numbers and distribution are also similar to wt. Several proteins, involved in endocytosis and membrane trafficking have been implicated in SV biogenesis at the nerve terminal (Hannah *et al.*, 1999). By virtue of its localization on SVs and its functions as a vesicular neurotransmitter transporter, it was reasonable to hypothesize that VMAT2 might also be involved in SV biogenesis. Indeed, a subset of excitatory terminals in mice lacking VGLUT1, a functionally related vesicular neurotransmitter transporter for glutamate, show a severe reduction in both total and reserve pool SV numbers, implicating VGLUT1 in SV biogenesis (Fremeau *et al.*, 2004). In contrast, our findings indicate that VMAT2 is not required for the biogenesis or the normal distribution of SVs, pointing toward fundamental, previously unsuspected, differences between SV biogenesis in glutamate and DA neurons. Interestingly, changes in the levels of several synaptic proteins, such as synapsin, a SV protein intimately involved in reserve pool mobilization (Pieribone *et al.*, 1995), were detected in the brains of VGLUT1 KO mice. Whether the marked decrease in synapsin levels, in the VGLUT1 KOs, is implicated in the reduction in reserve pool vesicle numbers, remains to be determined. Further, it is currently not known whether similar changes in protein levels occur in the brains of VMAT2 KO animals.

Our data also indicate that SV exocytosis and endocytosis are independent of the level of SV filling with transmitter. Consistent with our observations, Tabares *et al.* (2001) showed that, in chromaffin cells, the depletion of transmitter from secretory granules did not prevent their exocytosis. What's more, Travis *et al.* (2000) showed that mast cell secretory granules from VMAT2 KO mice were capable of stimulation-dependent exocytosis, despite the complete absence of transmitter release. However, unlike the DA neurons that we studied, mast cells normally express VMAT2 on secretory granules that contain 5-HT and histamine and are formed at the Golgi, much like the LDCVs described above. Our findings are also supported by other studies in which the uptake of transmitter by SVs was inhibited pharmacologically. For example, when the uptake of acetylcholine (ACh) into the SV at the snake NMJ was blocked by the vesicular ACh transporter (VAChT) inhibitor vesamicol, SVs continued to cycle (Parsons *et al.*, 1999). Similarly, SVs continued to cycle in rat hippocampal neurons after exposure to bafilomycin A, a compound that specifically blocks the vacuolar-type ATPase responsible for creating the energy gradient that drives vesicular neurotransmitter uptake (Zhou *et al.*, 2000). Our results extend these observations by showing for the first time that, in DA neurons, SVs can cycle not only in the absence of filling per se, but also in the complete absence of the vesicular transporter protein responsible for the filling. These data are also consistent with recent work showing that FM1-43 staining and destaining were unaltered in cultured hippocampal neurons from VGLUT1 KO mice (Wojcik *et al.*, 2004).

In view of our findings that VMAT2 does not influence the total number of SVs or their ability to cycle, modulations of VMAT2 levels at the synapse may influence the amount of DA available for release by affecting the proportion of SVs that bear VMAT2 and that are able to fill with DA. The SVs that we characterized in the present study were observed in KO animals, which represent an extreme scenario, incompatible with prolonged survival. However, more modest changes in VMAT2 levels also appear to change not only the amount of DA released by each SV, but also the number of SVs that are capable of releasing DA (Reimer *et al.*, 1998). For instance, when SVs are allowed to fill to thermodynamic equilibrium in unstimulated DA neurons cultured from VMAT2 heterozygous mice in which VMAT2 expression is

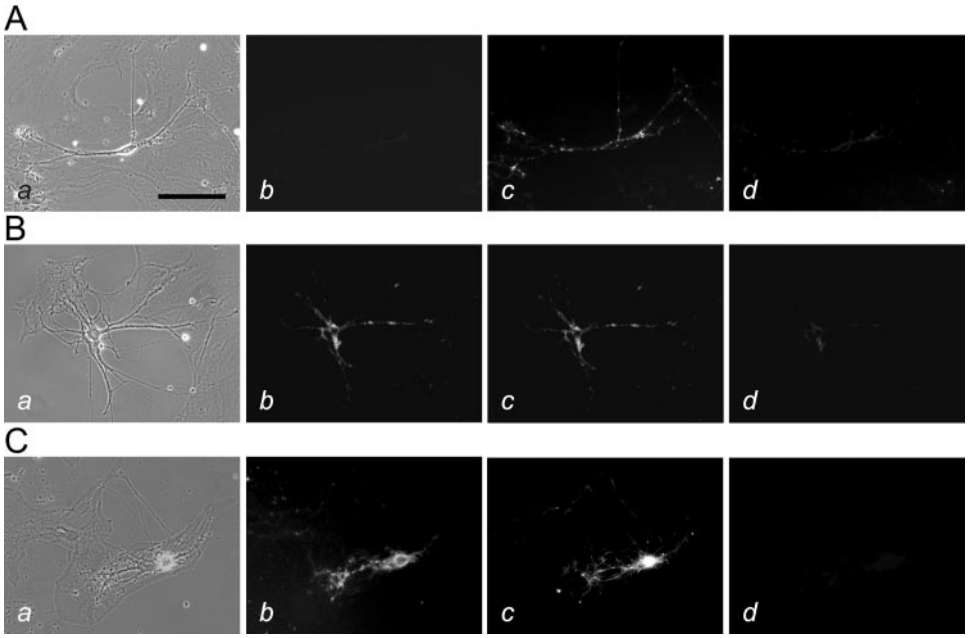

Figure 6. Specificity of FM1-43 staining in cultured neurons. (A) Mock-staining: A representative phase contrast image of a neuron (a) from a culture that was exposed to FM1-43 in the absence of depolarization. The neuron did not demonstrate any nonspecific FM1-43 fluorescence (b). Subsequent FM1-43 staining (c) and destaining (d) of the same neuron confirmed its viability. (B) Mock-destaining: a representative phase contrast image of a neuron (a) from a culture showing that FM1-43 fluorescence did not decrease nonspecifically during the course of the uptake experiment (b = 2 min; c = 30 min) but decreased rapidly after exposure to high-potassium buffer (d). (C) Residual FM1-43: A representative phase contrast image of a neuron (a) from a culture that was stained with FM1-43 (b; red) and immediately processed for TH immunofluorescence (c; green) showing that FM1-43 did not produce any residual fluorescence (d; red). Scale bar, 10 μm.

reduced by half, they accumulate only ~65% as much DA as cultures from wt mice, suggesting that fewer SVs are able to store DA (Fon *et al.*, 1997). Similarly, when VMAT2 expression is reduced by ~95% as in the KA1 VMAT2 mutant mice, electrically stimulated DA release is reduced to ~30% of wt levels (Patel *et al.*, 2003). Conversely, the overexpression of VMAT2 in cultured DA neurons allows more SVs to store and release DA, resulting in an increased frequency of release events upon stimulation (Pothos *et al.*, 2000). Our results suggest that the above changes do not reflect changes in the absolute number of SVs, but rather changes in the proportion of SVs that carry VMAT2. Hence, when SVs cycle at the plasma membrane, it is possible that certain SVs incorporate a VMAT2 molecule during endocytosis whereas others will not (i.e., remain empty), depending on the local availability of transporter. The current study therefore provides an important proof of principle, that empty SVs can exist and cycle. It remains to be determined whether such a pool of empty SVs also exists in the context of physiological VMAT2 levels.

VMAT2 levels are regulated transcriptionally and can be modulated by stimuli such as sustained neural activity and

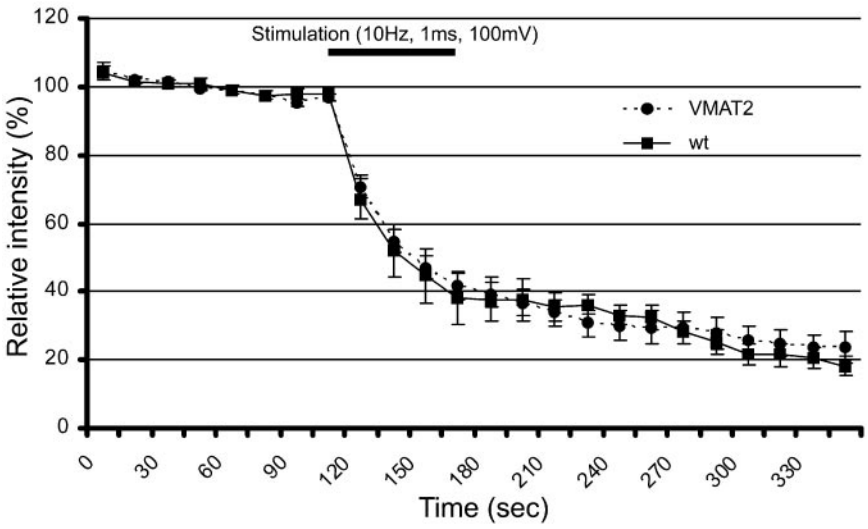

Figure 7. DA neurons from VMAT2 KO mice display the same SV cycling kinetics as those derived from wt mice. The rate of FM2-10 destaining in TH-positive neurons, as measured by the decrease in fluorescence intensity over time after electrical field stimulation, is shown. No differences were seen between TH-positive neurons derived from VMAT2 KO compared with those from derived from wt mice. One hundred ten terminals from 5 VMAT2 KO neurons and 86 terminals from 4 wt neurons were examined. Error bars, SEM.

psychostimulant drugs (Desnos *et al.*, 1995; Watson *et al.*, 1999; Fleckenstein *et al.*, 2000; Richardson and Miller, 2004). Further, pharmacological manipulations that alter DA concentrations in vivo have also been shown to change VMAT2 protein levels (Zucker *et al.*, 2001). Beyond the regulation of absolute levels, VMAT2 trafficking may also modulate its presence on SVs. Both phosphorylation and a di-leucine motif in the VMAT2 carboxy-terminus, involved in VMAT2 endocytosis and trafficking in secretory cells (Krantz *et al.*, 1997; Tan *et al.*, 1998; Waites *et al.*, 2001), may similarly regulate VMAT2 trafficking at the synapse and its incorporation into SVs (Fon and Edwards, 2001). Indeed, acute administration of psychostimulants in rats, a treatment that significantly alters DA transmission, appears to result in the redistribution of VMAT2 to distinct membrane compartments within synaptic terminals (Riddle *et al.*, 2002).

Taken together with our results, these studies suggest that neurons may modulate the distribution of VMAT2 on SVs in response to stimuli that can influence DA synaptic transmission. Further, the results suggest that the expression of VMAT2 on SVs could modulate the state of SVs from functionally empty to fillable, thereby representing an important point of regulation in DA transmission.

ACKNOWLEDGMENTS

We thank Mariette Houle, Anne Morinville, France Moreau, Marie-Josee Bourque, Noura Labib, and Sophie-Anne Lamour for technical assistance. We thank Dr. Thomas Stroh for assistance with the figures. This work was supported by an Operating Grant from the CIHR (MOP-42457). E.A.F. is supported by a CIHR Clinician Scientist Award phase 2. L.-E.T. is supported by a FRSQ (Québec) salary award and by a CIHR operating grant. B.G.C. is supported by a Jeanne-Timmins Costello Studentship from the MNI. G.D.F. is supported in part by studentship from the Fonds dela Recherche en Santé du Québec and the Natural Sciences and Engineering Research Council of Canada.

REFERENCES

Bekkers, J. M., Richerson, G. B., and Stevens, C. F. (1990). Origin of variability in quantal size in cultured hippocampal neurons and hippocampal slices. Proc. Natl. Acad. Sci. USA *87*, 5359–5362.

Bekkers, J. M., and Stevens, C. F. (1991). Excitatory and inhibitory autaptic currents in isolated hippocampal neurons maintained in cell culture. Proc. Natl. Acad. Sci. USA *88*, 7834–7838.

Bergevin, A., Girardot, D., Bourque, M. J., and Trudeau, L. E. (2002). Presynaptic mu-opioid receptors regulate a late step of the secretory process in rat ventral tegmental area GABAergic neurons. Neuropharmacology *42*, 1065–1078.

Boudin, H., Pelaprat, D., Rostene, W., Pickel, V. M., and Beaudet, A. (1998). Correlative ultrastructural distribution of neurotensin receptor proteins and binding sites in the rat substantia nigra. J. Neurosci. *18*, 8473–8484.

Bourque, M. J., and Trudeau, L. E. (2000). GDNF enhances the synaptic efficacy of dopaminergic neurons in culture. Eur. J. Neurosci. *12*, 3172–3180.

Bruns, D., Riedel, D., Klingauf, J., and Jahn, R. (2000). Quantal release of serotonin. Neuron *28*, 205–220.

Chan, J., Aoki, C., and Pickel, V. M. (1990). Optimization of differential immunogold-silver and peroxidase labeling with maintenance of ultrastructure in brain sections before plastic embedding. J. Neurosci. Methods *33*, 113–127.

Chuhma, N., Zhang, H., Masson, J., Zhuang, X., Sulzer, D., Hen, R., and Rayport, S. (2004). Dopamine neurons mediate a fast excitatory signal via their glutamatergic synapses. J. Neurosci. *24*, 972–981.

Cochilla, A. J., Angleson, J. K., and Betz, W. J. (1999). Monitoring secretory membrane with FM1-43 fluorescence. Annu. Rev. Neurosci. *22*, 1–10.

Colliver, T. L., Pyott, S. J., Achalabun, M., and Ewing, A. G. (2000). VMAT-mediated changes in quantal size and vesicular volume. J. Neurosci. *20*, 5276–5282.

Congar, P., Bergevin, A., and Trudeau, L. E. (2002). D2 receptors inhibit the secretory process downstream from calcium influx in dopaminergic neurons: implication of K+ channels. J. Neurophysiol. *87*, 1046–1056.

Dal Bo, G., St-Gelais, F., Danik, M., Williams, S., Cotton, M., and Trudeau, L. E. (2004). Dopamine neurons in culture express VGLUT2 explaining their capacity to release glutamate at synapses in addition to dopamine. J. Neurochem. *88*, 1398–1405.

Desnos, C., Laran, M. P., Langley, K., Aunis, D., and Henry, J. P. (1995). Long term stimulation changes the vesicular monoamine transporter content of chromaffin granules. J. Biol. Chem. *270*, 16030–16038.

Fleckenstein, A. E., Gibb, J. W., and Hanson, G. R. (2000). Differential effects of stimulants on monoaminergic transporters: pharmacological consequences and implications for neurotoxicity. Eur. J. Pharmacol. *406*, 1–13.

Fon, E. A., and Edwards, R. H. (2001). Molecular mechanisms of neurotransmitter release. Muscle Nerve *24*, 581–601.

Fon, E. A., Pothos, E. N., Sun, B. C., Killeen, N., Sulzer, D., and Edwards, R. H. (1997). Vesicular transport regulates monoamine storage and release but is not essential for amphetamine action. Neuron *19*, 1271–1283.

Fremeau, R. T., Jr. *et al.* (2002). The identification of vesicular glutamate transporter 3 suggests novel modes of signaling by glutamate. Proc. Natl. Acad. Sci. USA *99*, 14488–14493.

Fremeau, R. T., Jr., Kam, K., Qureshi, T., Johnson, J., Copenhagen, D. R., Storm-Mathisen, J., Chaudhry, F.A., Nicoll, R.A., and Edwards, R.H. (2004). Vesicular glutamate transporters 1 and 2 target to functionally distinct synaptic release sites. Science *304*, 1815–1819.

Fremeau, R. T., Jr., Troyer, M. D., Pahner, I., Nygard, D. O., Tran, C. H., Reimer, R. J., Bellocchio, E.. E., Fortin, D., Storm-Mathisen, J., and Edwards, R. H. (2001). The expression of vesicular glutamate transporters defines two classes of excitatory synapse. Neuron *31*, 247–260.

Gras, C., Herzog, E., Bellenchi, G. C., Bernard, V., Ravassard, P., Pohl, M., Gasnier, B., Giros, B., and El Mestikawy, S. (2002). A third vesicular glutamate transporter expressed by cholinergic and serotoninergic neurons. J. Neurosci. *22*, 5442–5451.

Greengard, P. (2001). The neurobiology of slow synaptic transmission. Science *294*, 1024–1030.

Hannah, M. J., Schmidt, A. A., and Huttner, W. B. (1999). Synaptic vesicle biogenesis. Annu. Rev. Cell Dev. Biol. *15*, 733–798.

Herzog, E., Bellenchi, G. C., Gras, C., Bernard, V., Ravassard, P., Bedet, C., Gasnier, B., Giros, B., and El Mestikawy, S. (2001). The existence of a second vesicular glutamate transporter specifies subpopulations of glutamatergic neurons. J. Neurosci. *21*, RC181.

Herzog, E., Gilchrist, J., Gras, C., Muzerelle, A., Ravassard, P., Giros, B., Gaspar, P., and El Mestikawy, S. (2004). Localization of VGLUT3, the vesicular glutamate transporter type 3, in the rat brain. Neuroscience *123*, 983–1002.

Krantz, D. E., Peter, D., Liu, Y., and Edwards, R. H. (1997). Phosphorylation of a vesicular monoamine transporter by casein kinase II. J. Biol. Chem. *272*, 6752–6759.

Michel, F. J., and Trudeau, L. E. (2000). Clozapine inhibits synaptic transmission at GABAergic synapses established by ventral tegmental area neurones in culture. Neuropharmacology *39*, 1536–1543.

Mooslehner, K. A., Chan, P. M., Xu, W., Liu, L., Smadja, C., Humby, T., Allen, N. D., Wilkinson, L. S., and Emson, P. C. (2001). Mice with very low expression of the vesicular monoamine transporter 2 gene survive into adulthood: potential mouse model for parkinsonism. Mol. Cell. Biol. *21*, 5321–5331.

Nicola, S. M., Surmeier, J., and Malenka, R. C. (2000). Dopaminergic modulation of neuronal excitability in the striatum and nucleus accumbens. Annu. Rev. Neurosci. *23*, 185–215.

Nirenberg, M. J., Chan, J., Liu, Y., Edwards, R. H., and Pickel, V. M. (1997). Vesicular monoamine transporter-2, immunogold localization in striatal axons and terminals. Synapse *26*, 194–198.

Parsons, R. L., Calupca, M. A., Merriam, L. A., and Prior, C. (1999). Empty synaptic vesicles recycle and undergo exocytosis at vesamicol-treated motor nerve terminals. J. Neurophysiol. *81*, 2696–2700.

Patel, J., Mooslehner, K. A., Chan, P. M., Emson, P. C., and Stamford, J. A. (2003). Presynaptic control of striatal dopamine neurotransmission in adult vesicular monoamine transporter 2 (VMAT2) mutant mice. J. Neurochem. *85*, 898–910.

Pieribone, V. A., Shupliakov, O., Brodin, L., Hilfiker-Rothenfluh, S., Czernik, A. J., and Greengard, P. (1995). Distinct pools of synaptic vesicles in neurotransmitter release. Nature *375*, 493–497.

Pothos, E. N., Larsen, K. E., Krantz, D. E., Liu, Y., Haycock, J. W., Setlik, W., Gershon, M. D., Edwards, R. H., and Sulzer, D. (2000). Synaptic vesicle transporter expression regulates vesicle phenotype and quantal size. J. Neurosci. *20*, 7297–7306.

Rayport, S., Sulzer, D., Shi, W. X., Sawasdikosol, S., Monaco, J., Batson, D., and Rajendran, G. (1992). Identified postnatal mesolimbic dopamine neurons in culture: morphology and electrophysiology. J. Neurosci. *12*, 4264–4280.

Reimer, R. J., Fon, E. A., and Edwards, R. H. (1998). Vesicular neurotransmitter transport and the presynaptic regulation of quantal size. Curr. Opin. Neurobiol. *8*, 405–412.

Richardson, J. R., and Miller, G. W. (2004). Acute exposure to aroclor 1016 or 1260 differentially affects dopamine transporter and vesicular monoamine transporter 2 levels. Toxicol. Lett. *148*, 29–40.

Riddle, E. L., Topham, M. K., Haycock, J. W., Hanson, G. R., and Fleckenstein, A. E. (2002). Differential trafficking of the vesicular monoamine transporter-2 by methamphetamine and cocaine. Eur. J. Pharmacol. *449*, 71–74.

Schafer, M. K., Varoqui, H., Defamie, N., Weihe, E., and Erickson, J. D. (2002). Molecular cloning and functional identification of mouse vesicular glutamate transporter 3 and its expression in subsets of novel excitatory neurons. J. Biol. Chem. *277*, 50734–50748.

Schikorski, T., and Stevens, C. F. (2001). Morphological correlates of functionally defined synaptic vesicle populations. Nat. Neurosci. *4*, 391–395.

Staple, J. K., Osen-Sand, A., Benfenati, F., Pich, E. M., and Catsicas, S. (1997). Molecular and functional diversity at synapses of individual neurons in vitro. Eur. J. Neurosci. *9*, 721–731.

Sudhof, T. C. (2000). The synaptic vesicle cycle revisited. Neuron *28*, 317–320.

Sulzer, D., Joyce, M. P., Lin, L., Geldwert, D., Haber, S. N., Hattori, T., and Rayport, S. (1998). Dopamine neurons make glutamatergic synapses in vitro. J. Neurosci. *18*, 4588–4602.

Tabares, L., Ales, E., Lindau, M., and Alvarez de Toledo, G. (2001). Exocytosis of catecholamine (CA)-containing and CA-free granules in chromaffin cells. J. Biol. Chem. *276*, 39974–39979.

Takahashi, N., Miner, L. L., Sora, I., Ujike, H., Revay, R. S., Kostic, V., Jackson-Lewis, V., Przedborski, S., and Uhl, G. R. (1997). VMAT2 knockout mice: heterozygotes display reduced amphetamine-conditioned reward, enhanced amphetamine locomotion, and enhanced MPTP toxicity. Proc. Natl. Acad. Sci. USA *94*, 9938–9943.

Tan, P. K., Waites, C., Liu, Y., Krantz, D. E., and Edwards, R. H. (1998). A leucine-based motif mediates the endocytosis of vesicular monoamine and acetylcholine transporters. J. Biol. Chem. *273*, 17351–17360.

Travis, E. R., Wang, Y. M., Michael, D. J., Caron, M. G., and Wightman, R. M. (2000). Differential quantal release of histamine and 5-hydroxytryptamine from mast cells of vesicular monoamine transporter 2 knockout mice. Proc. Natl. Acad. Sci. USA *97*, 162–167.

Van der Kloot, W., Molgo, J., Cameron, R., and Colasante, C. (2002). Vesicle size and transmitter release at the frog neuromuscular junction when quantal acetylcholine content is increased or decreased. J. Physiol. *541*, 385–393.

Varoqui, H., Schafer, M. K., Zhu, H., Weihe, E., and Erickson, J. D. (2002). Identification of the differentiation-associated Na+/PI transporter as a novel vesicular glutamate transporter expressed in a distinct set of glutamatergic synapses. J. Neurosci. *22*, 142–155.

Waites, C. L., Mehta, A., Tan, P. K., Thomas, G., Edwards, R. H., and Krantz, D. E. (2001). An acidic motif retains vesicular monoamine transporter 2 on large dense core vesicles. J. Cell Biol. *152*, 1159–1168.

Wang, Y. M., Gainetdinov, R. R., Fumagalli, F., Xu, F., Jones, S. R., Bock, C. B., Miller, G. W., Wightman, R.M., and Caron, M. G. (1997). Knockout of the vesicular monoamine transporter 2 gene results in neonatal death and supersensitivity to cocaine and amphetamine. Neuron *19*, 1285–1296.

Watson, F., Deavall, D. G., Macro, J.A., Kiernan, R., and Dimaline, R. (1999). Transcriptional activation of vesicular monoamine transporter 2 in the pre-B cell line Ea3.123. Biochem. J. *337*(Pt 2), 193–199.

Wojcik, S. M., Rhee, J. S., Herzog, E., Sigler, A., Jahn, R., Takamori, S., Brose, N., and Rosenmund, C. (2004). An essential role for vesicular glutamate transporter 1 (VGLUT1) in postnatal development and control of quantal size. Proc. Natl. Acad. Sci. USA *101*, 7158–7163.

Zhang, B., Koh, Y. H., Beckstead, R. B., Budnik, V., Ganetzky, B., and Bellen, H. J. (1998). Synaptic vesicle size and number are regulated by a clathrin adaptor protein required for endocytosis. Neuron *21*, 1465–1475.

Zhou, Q., Petersen, C. C., and Nicoll, R. A. (2000). Effects of reduced vesicular filling on synaptic transmission in rat hippocampal neurones. J. Physiol. *525*(Pt 1), 195–206.

Zucker, M., Weizman, A., Harel, D., and Rehavi, M. (2001). Changes in vesicular monoamine transporter (VMAT2) and synaptophysin in rat Substantia nigra and prefrontal cortex induced by psychotropic drugs. Neuropsychobiology *44*, 187–191.